

Rooted Spiral Trees on Hyper-cubic lattices

Sumedha*

Department Of Theoretical Physics
Tata Institute Of Fundamental Research
Homi Bhabha Road, Mumbai 400005
India

Abstract

We study rooted spiral trees in 2,3 and 4 dimensions on a hyper cubic lattice using exact enumeration and Monte-Carlo techniques. On the square lattice, we also obtain exact lower bound of 1.93565 on the growth constant λ . Series expansions give $\theta = -1.3667 \pm 0.0010$ and $\nu = 0.6574 \pm 0.0010$ on a square lattice. With Monte-Carlo simulations we get the estimates as $\theta = -1.364 \pm 0.010$, and $\nu = 0.656 \pm 0.010$. These results are numerical evidence against earlier proposed dimensional reduction by four in this problem. In dimensions higher than two, the spiral constraint can be implemented in two ways. In either case, our series expansion results do not support the proposed dimensional reduction.

Keywords: Spiral trees, Exact enumeration, Dimensional reduction

Spiral structures are very common in nature. Some examples of the beautiful spiral structures in galaxies, shoot arrangement in plants, polymers with spiral structure etc may be found in the book by Hargittai [1]. In statistical mechanics, lattice models of spiral self avoiding walks have been studied and can be solved exactly in two dimension [2, 3], though no solution is known for the self avoiding walks without the spiral constraint. A model of spiral trees and animals was proposed by Li and Zhou [4], which based on numerical studies was suggested to be in a new universality class. This problem was further studied by Bose et. al [5]. Based on the numerical evidence, and guided by the fact that magnetic field acting perpendicular to the motion of a charged particle produces spiralling motion and reduction by two in effective dimensionality, they conjectured that

*sumedha@theory.tifr.res.in

spiral tree problem would show a dimensional reduction by four. They conjectured the exponents of the spiral tree problem follow the following relations

$$\theta = (d - 4)\nu_{pl} \text{ for } d = 2 \quad (1)$$

$$\theta = (d - 4)\nu_{\perp} \text{ for } d > 2 \quad (2)$$

where θ is the entropic exponent and ν_{pl} and ν_{\perp} are the exponents related to the radius of gyration in the plane in which the tree has a rotational constraint and perpendicular to that plane respectively.

Since then this problem has not been studied further. Dimensional reduction is an intriguing possibility. The lattice tree model without spiral constraint is known to show a dimensional reduction by two [6]. The directed version, show a dimensional reduction by one. For both models, the tree and animals are believed to lie in the same universality class. In this paper, we revisit the problem and obtain a significantly longer series for rooted spiral trees. Specifically in two dimensions we have added twelve terms to the earlier series of 25 terms. In three and four dimensions, we generated a seventeen and a thirteen term series respectively. The earlier known series in three and four dimensions had thirteen and nine terms. In the process, we also correct some mistakes in the earlier reported series. We also perform Monte-Carlo (MC) simulations using the improved incomplete enumeration algorithm [7] and generate spiral trees up to sizes of 1000 in two dimensions. Our analysis of exact series and MC samples do not support the conjectured dimensional reduction by four in this problem.

A lattice tree is a cluster of connected sites which contains no loops. Spiral trees are a subclass of lattice trees. In a tree every cluster site is attached to the origin through a unique path. In a spiral tree, this path has a specific rotational constraint.

We define rooted spiral tree as a acyclic connected subgraph of a lattice such that the projection of the path joining any site of the tree to the root on $x - y$ plane contains no left turn (Fig. 1). We will measure the size of a spiral tree by the number of sites present in the tree. These are called spiral site trees. The number of possibilities of spiral bond trees are more than that for spiral site trees but both are thought to lie in the same universality class. For example, the site marked as X in Fig.1 is not allowed in spiral site

tree as it would introduce a loop. But it can be present in a spiral bond tree.

Let the total number of distinct rooted spiral trees be A_n . This is expected to have a asymptotic behaviour of the form

$$A_n \sim C\lambda^n n^{-\theta} \quad (3)$$

where C is a constant, θ is a critical exponent and is expected to depend only on the dimension of the lattice and λ is known as the lattice dependent growth constant. The existence of growth constant λ for unrooted lattice trees and animals has been proved rigorously using concatenation and super multiplicity arguments [8]. Also a rigorous lower bound for θ for unrooted lattice trees and animals has been proved [9] using pattern theorem. Specifically, it is $\theta \geq (d-1)/d$, for any dimension $d \geq 2$. Eq. 3 is expected to hold for most cluster enumeration problems on regular lattices, though other asymptotic forms are also possible. For example, for spiral self-avoiding walks on square and triangular lattices, A_n tends to a stretched exponential in n in the asymptotic limit [2, 3]. Though we do not prove existence of λ and θ for spiral trees in this paper, we derive a lower bound for λ . Also, since spiral trees are a subset of lattice trees, $\lambda_{spiral} \leq \lambda_{all}$, where λ_{all} is the growth constant for all trees, $\lambda_{all} \approx 3.795$ on a square lattice [10]. In two dimensions, we have derived the generating function for enumeration of a subset of all possible spiral trees. The value of growth constant for this subset is 1.93565. This gives a lower bound on the growth constant λ_{spiral} of the spiral trees on a square lattice. This bound will be derived in Section 1.1.

For the conventional lattice animals, one can prove $\theta \geq 0$ through concatenation and super-multiplicity arguments [8, 9]. Concatenation does not work for spiral trees. Interestingly, our numerical studies give a negative value of θ in two and three dimensions.

The spiral trees are anisotropic. We measure the average extent of a n -site spiral tree in $x-y$ plane and perpendicular to the $x-y$ plane through the moment of inertia tensors, $I_{pl,n}$ and $I_{\perp,n}$ respectively. In the asymptotic limit, they are expected to vary as

$$I_{pl,n} \sim A n^{2\nu_{pl}+1} \quad (4)$$

and

$$I_{\perp,n} \sim A n^{2\nu_{\perp}+1} \quad (5)$$

where ν_{pl} and ν_{\perp} define the length scale of the spiral tree in planar and perpendicular direction respectively.

1 Two dimensional lattice spiral trees

Some pictures of randomly generated large spiral trees are shown in Fig. 2 (details later). One notes very long one dimensional structures with infrequent turns. Hence, simple counting of structures of kind shown in Fig.3 should give a good estimate of the growth constant λ . The generating function of trees of this type is easy to determine. If $A_1(x)$ is the generating function, we get

$$A_1(x) = \frac{x}{1-x} + \frac{x^3}{(1-x)^2} A_1(x) \quad (6)$$

which gives $A_1(x) = \frac{x(1-x)}{1+x^2-2x-x^3}$. The number of trees of this type grows as λ_1^n , with $\lambda_1 = 1.754878$. It is straightforward to include more complicated branches in such counting to get a better lower bound. This we proceed to do below.

1.1 Lower Bound on Growth Constant on Square lattice

Consider a subset of all the spiral trees on a square lattice rooted at the origin, which lie strictly in the first quadrant $x \geq 0, y \geq 0$; starting at the origin, and not touching $y = 0$ and $y = 1$ except at points $(0,0)$ and $(0,1)$ respectively. If $Q(x)$ is the generating function for spiral trees in a quadrant and if $q_{4,n}$ is the coefficient of x^n in the expansion of $([Q(x)]^4)/x^3$, then

$$A_n \geq q_{4,n} \quad (7)$$

where A_n is the n^{th} term of $A(x)$, the generating function of all spiral trees on the square lattice.

The enumeration of graphs contributing to $Q(x)$ can be made easier by noticing that these graphs can be formed by combination of smaller graphs. We define an articulation point [11] as a point on y -axis such that the tree above is an allowed spiral tree in the

quadrant above that part (note that these trees are defined in the upper quadrant and they never touch $y = 0$ axis, except at $(0,0)$). For example, the solid squares represent the articulation points of the graph in Fig. 3, and Fig.4 shows a spiral tree with no articulation point. Hence, these spiral trees can be seen as trees having y axis as a backbone on which spiral graphs are connected at different articulation points maintaining the spiral constraint.

Let $B(x)$ be the generating function of the quadrant spiral trees with no articulation points. Hence $B(x)$ can be seen as sum of generating function of irreducible graphs with i sites along y -axis. We represent them by $B_i(x)$ (see Fig. 5), then $B(x) = \sum_{i=1}^{\infty} B_i(x)$. The full generating function in terms of $B(x)$ would be

$$Q(x) = x(1 + B(x) + B^2(x) + \dots) = \frac{x}{1 - B(x)} \quad (8)$$

where $B_i(x)$ are spiral graphs starting with i -sites along the y -axis. It is easy to see that $B_1(x) = x$, $B_2(x) = \frac{x^3}{1-x}$ and $B_3(x) = \frac{x^6}{(1-x-x^3)(1-x)}$. One can write $B_4(x)$ with some effort but we do not have a general form for $B_i(x)$ for any i .

We restrict the graphs contributing to $B_i(x)$ to be graphs such that they have i sites along the y axis and have at least one downward branch with $i - 1$ sites. This would not include structures like Fig. 4. We will represent the generating function of these graphs by $Q_1(x)$. Then we can represent $B_i(x)$ in terms of two other generating functions, $V_i(x)$ and $W_i(x)$. We define $V_i(x)$ as the generating function of spiral subgraphs starting with having i sites along y -axis. $W_i(x)$ is the generating function of spiral subgraphs starting with i -sites along y -axis and ending with a downward branch with $i - 1$ sites (Fig.6). Then,

$$B_i(x) = W_i(x) + \frac{W_i(x)V_{i-1}(x)}{x^{i-1}} \quad (9)$$

Also, $V_i(x)$ can be rewritten in terms of $W_i(x)$ as

$$V_i(x) = xV_{i-1}(x) + W_i(x) + \frac{W_i(x)V_{i-1}(x)}{x^{i-1}} \quad (10)$$

By expressing $Q_1(x)$ in terms of $B_i(x)$ and $B_i(x)$ in turn in terms of $W_i(x)$, we can reduce the computational time. If W_n is the number of graphs of size n contributing to

$W(x)$ ($W(x) = \sum_{i=1}^{\infty} W_i(x)$), and Q_n is the number of graphs of size n contributing to $Q_1(x)$, then W_n grows more slowly than Q_n . We enumerated W_n and using them we could generate a 56 term series for $Q_1(x)$. The computation time for W_n grows as $(1.8)^n$, in contrast to $(2.04)^n$ for the Q_n series.

If we restrict the graphs contributing to $B_i(x)$, $W_i(x)$ and $V_i(x)$ to the graphs having comb-like structure (by comb-like structure we mean graphs with one dimensional backbone having vertical straight lines of arbitrary lengths), then it turns out that one can get the exact expression for these generating functions. We represent them by $\tilde{V}_i(x)$, $\tilde{W}_i(x)$ and $\tilde{B}_i(x)$. It is easy to see that for comb like structures,

$$W_i(x) \geq \tilde{W}_i(x) = \frac{x^{2i}}{1-x} + \frac{x^{2i}}{1-x} \frac{K(x)}{1-x} + \frac{x^{2i}}{1-x} \left(\frac{K(x)}{1-x} \right)^2 + \dots \quad (11)$$

where $K(x) = x^2 \sum_{j=1}^{i-2} x^j$. Hence,

$$\tilde{W}_i(x) = \frac{x^{2i}(1-x)}{1-2x+x^2-x^3+x^{i+1}} \quad (12)$$

Similarly, we get

$$\tilde{V}_i(x) = \frac{x^{i+1}(1-x+x^2-x^i)}{1-2x+x^2-x^3+x^{i+1}} \quad (13)$$

and hence

$$B_i(x) \geq \tilde{B}_i(x) = \frac{x^{2i}(1-x)^2}{(1-2x+x^2-x^3+x^i)(1-2x+x^2-x^3+x^{i+1})} \quad (14)$$

Substituting in Eq. 9 we get the generating function, $\tilde{Q}_1(x)$ for this subset of spiral trees in a quadrant. This generating function has a singularity at $x_c = 0.51662$ which gives the growth constant λ' of these trees to be 1.93565. Since this counts only a subset of all the spiral trees on a square lattice, this is a rigorous lower bound on λ_{spiral} for spiral trees on a square lattice.

For the full $Q_1(x)$, we derived a 56 term series. If we assume,

$$Q_n \sim \lambda_1^n n^{-\theta_1} \quad (15)$$

then we got estimates of λ_1 and θ_1 to be

$$\lambda_1 = 2.0449 \pm 0.0001 \quad (16)$$

$$\theta_1 = 0.830 \pm 0.01 \quad (17)$$

1.2 Exact enumeration

Since the number of configurations of a given cluster size is exponential in cluster size, the computational complexity of the algorithm for enumeration of all lattice animals or trees grows exponentially with the cluster size. For direct enumeration algorithms like Martin's algorithm [12], the time required to generate all the configurations of a given size grows as λ^n , where λ is the growth constant and n is the cluster size and the memory requirement grows like a polynomial in cluster size. For lattice trees and animals, a finite lattice method [13] with an associated transfer matrix algorithm was used by Conway [14]. Conway generated a 25 term series for lattice animals using this algorithm. This series has recently been extended to 46 terms by Jensen [10] with a slight improvement in the algorithm. Both space and time requirements of this algorithm are found numerically to approximately grow as 1.4^n . The growth constant of lattice animals in contrast is approximately 4.06. Hence a considerable improvement in time is obtained by the transfer matrix algorithm at the cost of memory.

The spiral constraint, cannot be easily implemented using the transfer matrix. Hence we have used Martin's algorithm for spiral trees, making use of the four-fold rotational symmetry of the lattice. Our series for number of trees and their average moment of inertia is given in Appendix.1.

Using this we generated a series of spiral trees on square lattice up to 37 terms (Appendix 1). Earlier known series had only 25 terms.

For analysing the series data we tried a four parameter sequential fit to the data of the form

$$A_n = B\lambda^n(n + \delta)^{-\theta} \quad (18)$$

where δ is an adjustable fixed parameter and B is a constant. We did a linear fit on the logarithm of Eq. 18 using A_n , A_{n+1} , A_{n+2} and A_{n+3} to estimate values of B_n , δ_n , λ_n and

θ_n . For spiral trees on square lattice we found a good convergence in successive values of λ_n and θ_n for δ lying between 2.03 and 2.04. Fixing $\delta = 2.0367$ and $B = 0.18124$ we get a very good convergence of λ_n and θ_n for different values of n . These are given in Appendix 2. From this we estimate

$$\lambda = 2.11433 \pm 0.00010 \quad (19)$$

$$\theta = -1.3667 \pm 0.0010 \quad (20)$$

We have tried fits with non analytic corrections to scaling of the form , $B\lambda^n(n+\delta)^{-\theta}[1+a/n^\Delta]$, but we didn't get good convergence for Δ . Instead, $B\lambda^n(n+\delta)^{-\theta}[1-\alpha e^{-\beta n}]$ seems to fit much better with $\alpha \approx 0.32$ and $\beta \approx 0.35$.

For the radius of gyration data we used a sequential fit of the form

$$\log I_{i,n} = (2\nu_i + 1)\ln(n + \delta) + u + \frac{v}{(n + \delta)^2} \quad (21)$$

where i stands for pl or \perp as the case maybe and u and v are constants.

For spiral trees in a plane $I_{\perp,n}$ would be zero and by symmetry the sum of square of x coordinate of all sites for all configurations of clusters of size n is symmetric with sum of squares of y -coordinate. Using Eq. 21 for sequential fit to our 35 term series we get a good convergence for δ lying between -0.33 and -0.35 . Fixing $\delta = -0.338$ we get the estimates of ν_{pl} to be

$$2\nu_{pl} = 1.3148 \pm 0.0010 \quad (22)$$

These estimates are much more precise than the earlier estimates $\lambda = 2.1166 \pm 0.001$, $\theta = -1.307 \pm 0.006$ and $2\nu_{pl} = 1.306 \pm 0.010$ using a 25 term series [5]. We can rule out the dimensional reduction conjecture with fair confidence.

Above we presented our estimates using four parameter fits. Method of differential approximants has almost become a standard technique for such analysis [15]. In this case, the generating function has a divergent singularity at x_c . We tried zeroth order differential approximants, they are listed in Table 1. We find a very poor convergence in values of x_c and θ . Out of 70 approximants, 15 show spurious singularities (singularities with

$|x_c| < 0.45$). We have listed 20 values which showed best convergence. From these we get, $\lambda = 2.1142 \pm 0.002$ and $\theta = -1.39 \pm 0.02$. Clearly the series is not very well behaved. This is reflected in the slow convergence of our series. Also Monte-Carlo generated random spiral trees of sizes 1000 (Fig. 2) suggest that the asymptotic behaviour of the series might set in rather late. Because of poor convergence of differential approximants, we have relied on parameter fits for series analysis in this paper.

1.3 Monte-Carlo analysis

With exact enumeration, we are restricted to clusters of size thirty seven in two dimensions. The main problem is with the extrapolation since the crossover sizes are likely to be large, as the total angle turned by the largest spiral arm about the origin for a spiral tree of size 1000 is about 2π only (Fig. 2). This indicates that the crossover value above which asymptotic behaviour sets in would be of order 10^3 . We tried to study larger spiral trees using MC methods. Monte-Carlo simulation of branched polymers is a challenging problem. Because of branching, most MC algorithms which are good for linear polymers show critical slowing down for branched polymers. For lattice trees there have been some studies using the cut and paste dynamic MC technique [9]. But with spiral constraint, algorithms involving large scale non local moves are not useful. We used an improved version of incomplete enumeration algorithm proposed recently by us [7]. Using it we could study spiral trees of sizes up to one thousand on a square lattice.

Incomplete enumeration is a simple modification of exact enumeration algorithm and can be seen as a percolation process on the genealogical tree of the underlying enumeration problem. The optimal behaviour of the algorithm is achieved when we work around the percolation threshold of the genealogical tree. This algorithm falls in the class of stochastic growth algorithm like PERM [16]. We have shown in [7], that the asymptotic time to produce an independent sample of n sites for trees and animals grows as $\exp(an^b)$ with $0 < b < 1$ for this algorithm. Though the coefficient in front of stretched exponential can be made small by optimising the algorithm for small sizes. We will not give more details of the algorithm in this paper. These can be found in [7].

Fig.2 shows pictures of some typical spiral trees of one thousand sites. Clearly, their structure is very different from lattice trees without the spiral constraint. Because of the

constraint they tend to branch much less. For spiral constraint, earlier numerical evidence suggest that unlike lattice trees and animals, spiral trees and animals do not lie in same universality class. The reason is that by allowing loops, the polymer can bend much more often and hence spiral animals would be more compact than the spiral trees.

We studied spiral trees up to sizes 1000 using incomplete enumeration MC method. We made 10^7 MC runs. The moment of inertia tensor $I_{pl,n}$ as a function of n is plotted in Fig 7 and Fig 8. Assuming the asymptotic form to be such that

$$\log(I_{pl,n}) = \log C + (2\nu_{pl} + 1)\log n + \frac{D}{n} \quad (23)$$

Using above written form, we get the estimate of ν_{pl} to be (Fig 7 and Fig 8)

$$2\nu_{pl} = 1.312 \pm 0.010 \quad (24)$$

In incomplete enumeration MC algorithm [7], each configuration of n sites is generated with equal probability P_n which is just $\prod_{i=1}^n p_i$, where p_i is the probability with which an edge between level i and $i + 1$ on the genealogical tree of the problem is chosen. By keeping track of the average number of clusters of a given size generated in a given run, one can estimate the growth constant λ and the critical exponent θ . But, the variance of the number of clusters increases as $\exp(n^\alpha)$, $0 < \alpha < 1$ for large n . Hence, instead we counted the number of descendants of each spiral tree generated. This approach has been used previously in [5, 17]. The mean number of descendants of a tree of size n gives a direct estimate of A_{n+1}/A_n . We represent the mean number of descendants by M_n . This is plotted in Fig. 9. A linear fit of the form $\lambda(1 - \theta/n)$ to this data gives $\lambda = 2.116 \pm 0.01$ and $\theta = -1.29 \pm 0.02$. For better estimates we assume

$$\log M_n = \log \lambda - \theta \log \left(\frac{n + \delta}{n - 1 + \delta} \right) \quad (25)$$

With this we get the following estimates for $n \leq 200$ which are in agreement with the value obtained by extrapolating the exact series expansions.

$$\lambda = 2.1145 \pm 0.0010 \quad (26)$$

$$\theta = -1.364 \pm 0.010 \quad (27)$$

with $\delta = 1.8$.

2 Spiral trees on a cubic lattice

In dimensions higher than two, the spiral constraint defined as the projection of path joining any site of the tree to the root in $x-y$ plane contains no left turn can be employed in two ways. Bose et. al. [5] defined it such that for the projected path from origin to site on $x-y$ plane only forward and right turns are allowed. But in dimensions higher than two, we can define another variation where trees as long as they do not violate the tree constraint and the projection on $x-y$ plane is spiral, are allowed. We will call the spiral trees with only forward and right turns allowed as ST_1 .

If we allow for back-turns also, we would get different series because for example, Fig 10 shows one spiral tree of six sites which would not be a valid configuration if we consider only forward and right turns. We call the spiral trees with back-turns allowed as ST_2 . Naively, one would expect these two to belong to the same universality class. We generated the series till $n = 17$ on a cubic lattice using both definitions, however we find the two series behaving differently. Series for both ST_1 and ST_2 are given in Appendix 1.

For ST_1 , for A_n the number of configurations, using Eq. 18 we find that the sequential fit shows a good convergence around $\delta = 2.43$. With $\delta = 2.43$ and $B = 0.094$, the values of λ and θ obtained are listed in Table 1. For ν_{pl} and ν_{\perp} , we used fitting form as given in Eq. 21, with $\delta = -1.46$ and $\delta = -0.43$ respectively. The sequential fits are given in Appendix 2 and estimates are listed in Table 2.

Similarly, we obtained 17 term series for ST_2 . The sequential fits are given in Appendix 2 and the values of λ , θ , ν_{pl} and ν_{\perp} are listed in Table 2.

The difference in value of λ for ST_1 and ST_2 is understandable as ST_2 has a greater number of configurations. More surprisingly, the critical exponents θ , ν_{pl} and ν_{\perp} within our error estimates are different in two models. In neither case, the conjectured dimensional reduction(Eq.1 and 2) seems to be satisfied.

3 Spiral trees in four dimensions

On a hyper cubic lattice in four dimensions we generated a series till $n = 13$. We also correct mistakes in the earlier series reported for ST_1 in [5]. The corrected series is given in the Appendix 1. We also obtained a 13 term series for ST_2 (see Appendix 1). The

estimates of λ and critical exponents are listed in Table 2.

We also performed Monte-Carlo simulations using incomplete enumeration algorithm for spiral trees up to size 50. Our estimates from MC simulations for ST_1 are given in Table 3.

Though we cannot rule out the possibility of θ being zero in both series analysis and Monte-Carlo simulations, but it seems unlikely.

4 Discussion

Bose et. al. gave a plausible argument of curling up of the dimensions in the spiralling plane and had conjectured a dimensional reduction by four for spiral trees. Our numerical evidence as presented in this paper does not support the conjecture. The spiral constraint for trees seems to be very special. For example, the structure of spiral trees is very different from spiral animals with loops allowed [18]. Different implementation of the constraint in $d > 2$, seems to give different critical behaviour, suggesting different universality classes. A variety of self avoiding walks with different step restrictions rules on simple cubic lattice were studied in [19] using exact enumeration. Their analysis suggested same universality class for self avoiding walks with various restrictions (including the spiral constraint), as the unrestricted self avoiding walks. In contrast, our studies show different critical behaviour of spiral trees with different geometrical restrictions in three and four dimensions.

We should note that for the large clusters of size 10^3 generated by Monte Carlo, the total angle turned by the largest spiral arm about the origin is about 2π . It is possible that the structure of spiral trees is such that this angle tends to infinity as n tends to infinity. In this case the crossover value above which asymptotic behaviour sets in would be expected to be of order 10^3 , and series analysis for smaller n may not give correct limiting behaviour. One indication that trees where spiral turns a lot are important is that the growth constant for spiral trees in a quadrant $Q_1(x)$ seems to be significantly smaller than for full spiral trees.

For quadrant spiral trees on a square lattice, we obtained exact series up to sizes 56. There are very few such long series known for lattice models. The series gives a estimate of $\lambda = 2.044$ for these quadrant spiral trees. This value is significantly smaller than for

the full spiral trees.

5 Acknowledgements

I am thankful to my adviser Prof. Deepak Dhar for suggesting the problem, for discussions and for useful comments on the manuscript.

6 Appendix 1

Exact series enumeration values in different dimensions

6.1 Two dimensions

cluster size(n)	A_n	$\langle I_{pl,n} \rangle$
1	1	0
2	4	1
3	14	3.142857
4	40	6.800000
5	105	12.266667
6	268	19.656716
7	674	28.919881
8	1660	40.159036
9	4021	53.513056
10	9612	69.074906
11	22734	86.926014
12	53276	107.140851
13	123916	129.787372
14	286376	154.926432
15	658100	182.624835
16	1504900	212.938547
17	3426464	245.919131
18	7771444	281.619675
19	17565064	320.089299
20	39576360	361.374917
21	88916877	405.522760
22	199252252	452.577078
23	445438310	502.580546
24	993616344	555.575100
25	2211923712	611.601183
26	4914811468	670.697934
27	10901498938	732.903853
28	24141259980	798.256392
29	53379537257	866.791847
30	117861710196	938.545859
31	259891311248	1013.553288
32	572356464452	1091.848086
33	1259008971656	1173.463504
34	2766351037428	1258.432171
35	6071954146120	1346.786006
36	13314252070412	
37	29167189621351	

6.2 Three Dimensions ST_1

n	A_n	$\langle I_{pl,n} \rangle$	$\langle I_{\perp,n} \rangle$
1	1	0.	0.
2	6	0.666666	0.333333
3	41	1.85366	1.07317
4	260	3.63076	2.27692
5	1568	6.02296	3.98214
6	9190	9.06464	6.19913
7	53090	12.75954	8.91987
8	303900	17.09588	12.1405
9	1727691	22.0606	15.8606
10	9767426	27.6424	20.0821
11	54966550	33.8322	24.8071
12	308138528	40.6214	30.0376
13	1721739000	48.0022	35.7754
14	9592901762	55.9676	42.0229
15	53314247488	64.5112	48.7822
16	295644339728	73.6274	56.0556
17	1636179620652	83.3112	63.8454

6.3 Three Dimensions ST_2

n	A_n	$\langle I_{pl,n} \rangle$	$\langle I_{\perp,n} \rangle$
1	1	0	0.
2	6	0.666666	0.333333
3	41	1.85366	1.07317
4	260	3.63076	2.27692
5	1576	6.00762	4.00761
6	9342	9.00192	6.30208
7	54890	12.60084	9.17041
8	320952	16.7848	12.6182
9	1869907	21.5398	16.651
10	10861750	26.8572	21.2772
11	62939998	32.7312	26.5047
12	364004296	39.156	32.3409
13	2101795408	46.1276	38.7927
14	12119643810	53.6422	45.8667
15	69805863940	61.6968	53.5693
16	401668665200	70.2898	61.9068
17	2309283532000	79.4192	70.8851

6.4 Four Dimensions ST_1

n	A_n	$\langle I_{pl,n} \rangle$	$\langle I_{\perp,n} \rangle$
1	1	0.	0
2	8	0.5	0.5
3	80	1.35	1.5
4	800	2.54	3.030
5	7912	4.05864	5.10010
6	77656	5.89816	7.70862
7	759172	8.04822	10.84584
8	7403292	10.49742	14.50268
9	72073417	13.23410	18.67008
10	700774524	16.24692	23.34
11	6806914432	19.52526	28.5052
12	66064406668	23.0592	34.1596
13	640741734643	26.8396	40.2974

6.5 Four dimensions ST_2

n	A_n	$\langle I_{pl,n} \rangle$	$\langle I_{\perp,n} \rangle$
1	1	0.	0.
2	8	0.5	0.5
3	80	1.35	1.5
4	800	2.54	3.030
5	7960	4.05226	5.10754
6	79048	5.87628	7.74208
7	785748	7.99822	10.93174
8	7822676	10.40506	14.6724
9	78011513	13.08484	18.95778
10	779189988	16.0274	23.7816
11	7793589943	19.22410	29.1376
12	78049537766	22.6676	35.0206
13	782489000000	26.3518	41.4252

7 Appendix 2

7.1 Two Dimensions Sequential Fit

n	λ_n	θ_n	$2\nu_{pl,n}$
5	2.078982187	-1.4143616	1.2918751
6	2.118727624	-1.3598402	1.3047319
7	2.117039314	-1.3623751	1.3092198
8	2.115352878	-1.3651395	1.3108492
9	2.114617151	-1.3664433	1.3117861
10	2.114771869	-1.3661493	1.312420
11	2.113813740	-1.3680905	1.3128895
12	2.113978775	-1.3677359	1.3132536
13	2.114183882	-1.3672706	1.3135423
14	2.114099443	-1.3674721	1.3137672
15	2.114103267	-1.3674625	1.3139586
16	2.114205656	-1.3671946	1.3141194
17	2.114223238	-1.3671466	1.3142505
18	2.114256310	-1.3670527	1.3143596
19	2.114279786	-1.3669834	1.3144497
20	2.114291286	-1.3669483	1.3145234
21	2.114301033	-1.3669174	1.3145839
22	2.114310834	-1.3668854	1.3146334
23	2.114311487	-1.3668832	1.3146734
24	2.114314464	-1.3668728	1.3147059
25	2.114318963	-1.3668566	1.3147321
26	2.114320428	-1.3668513	1.3147529
27	2.114321722	-1.3668464	1.3147694
28	2.114324605	-1.3668351	1.3147823
29	2.114326551	-1.3668274	1.3147921
30	2.114327932	-1.3668217	1.3147994
31	2.114329734	-1.3668142	1.3148047
32	2.114331349	-1.3668072	1.3148083
33	2.114332328	-1.3668029	1.3148104
34	2.114333055	-1.3667997	1.3148113
35	2.114333550	-1.3667974	1.3148113
36	2.114333553	-1.3667974	
Es. Val.	2.11433 ± 0.0001	-1.3667 ± 0.001	1.3148 ± 0.001

7.2 Three Dimensions ST_1

n	λ_n	θ_n	$2\nu_{pl,n}$	$2\nu_{\perp,n}$
5	5.153269	-1.019107	0.847865	1.128949
6	5.275382	-0.810187	0.865641	1.098419
7	5.310873	-0.743662	0.871330	1.083814
8	5.319667	-0.725590	0.874191	1.077873
9	5.327658	-0.707695	0.875922	1.073809
10	5.334141	-0.691977	0.876525	1.070550
11	5.337903	-0.682161	0.876502	1.068326
12	5.339533	-0.677605	0.876303	1.067085
13	5.340111	-0.675880	0.876176	1.066526
14	5.340282	-0.675339	0.876139	1.066334
15	5.340255	-0.675428	0.876197	1.066365
Es. Val.	5.340 ± 0.02	-0.675 ± 0.05	0.876 ± 0.05	1.066 ± 0.05

7.3 Three Dimensions ST_2

n	λ_n	θ_n	$2\nu_{pl,n}$	$2\nu_{\perp,n}$
5	5.694072	-0.143802	1.054721	1.200021
6	5.719085	-0.123718	1.013833	1.171160
7	5.710159	-0.132441	0.989310	1.153823
8	5.695471	-0.149408	0.977105	1.147515
9	5.689143	-0.157845	0.969817	1.144294
10	5.687350	-0.160552	0.963977	1.141637
11	5.686110	-0.162645	0.959561	1.139686
12	5.684763	-0.165153	0.956738	1.138646
13	5.683809	-0.167099	0.955250	1.138243
14	5.683473	-0.167843	0.954653	1.138124
15	5.683632	-0.167463	0.954662	1.138134
Es. Val.	5.683 ± 0.02	-0.167 ± 0.05	0.954 ± 0.05	1.138 ± 0.05

References

- [1] I Hargittai and C A Pickover eds. 1992, Spiral Symmetry, World Scientific, Singapore.
- [2] V Privman 1983, Spiral self-avoiding walks, J. Phys. A:Math. Gen **16** L571
- [3] A J Guttmann and N C Wormald 1984, On the number of spiral self-avoiding walks, J. Phys. A:Math. Gen. **17** 271

- [4] T C Li and Z C Zhou 1985, Spiral bond animals-ratio approach, J. Phys. A:Math. Gen. **18** 67
- [5] I Bose, P Ray and D Dhar 1988, Rooted spiral trees in dimensions 2,3 and 4,J. Phys. A:Math. Gen **21** L219
- [6] D C Brydges and J Z Imbrie 2003, Branched Polymers and Dimensional Reduction, Annals of Mathematics, **158** 1019
- [7] Sumedha and D Dhar 2004, Efficiency of the Incomplete Enumeration algorithm for Monte-Carlo simulation of linear and branched polymers, cond-mat/0408640 (submitted to J. Statistical Physics)
- [8] D J Klein 1981, Rigorous results for branched polymers with excluded volume, J. Chem. Phys. **75** 5186
- [9] N Madras 1995, A rigorous bound on the critical exponent for the number of lattice trees, animals and polygons, J. Stat. Phys. **78** 681
- [10] I Jensen 2001, Enumerations of lattice animals and trees, J. Stat. Phys. **102** 865.
- [11] J W Essam 1971, Percolation Processes.II, The Pair Connectedness, J. Math. Phys. **12** 874.
- [12] J. L. Martin 1974, Computer Techniques for Evaluating Lattice Constants, Phase Transitions and Critical Phenomena ,Eds. Domb and Green, vol. **3**.
- [13] I G Enting 1980, Generating functions for enumerating self-avoiding rings on the square lattice, J. Phys. A:Math. Gen. **13** 3713.
- [14] A Conway 1995, Enumerating $2D$ percolation series by finite-lattice method:theory J. Phys. A:Math. Gen. **28** 335.
- [15] D S Gaunt and A J Guttmann 1974, Asymptotic Analysis of Coefficients, Phase Transitions and Critical Phenomena ,Eds. Domb and Green, vol. **3**.

- [16] P Grassberger and W Nadler 2000, Go with the winners - Simulations, cond-mat/0010265, Proceedings der Heraeus-Ferientschule ”‘Vom Billiardtisch bis Monte Carlo: Spielfelder der statistischen Physik’”, Chemnitz, October 2000
- [17] E J Janse van Rensburg and A Rechnitzer 2003, High Precision canonical Monte Carlo determination of the growth constant of square lattice trees, Phys. Rev. E **67** 036116.
- [18] I Bose 2000, Lattice Animals and the Percolation Model under Rotational Constraint, Percolation Theory and Particle Systems, Eds. Rahul Roy, University Press, India.
- [19] A Rechnitzer and A L Owczarek 2000, On three-dimensional self-avoiding walk symmetry classes J. Phys. A:Math. Gen. **33** 2685.

Table Captions

1. Table1:Estimates of critical exponents and growth constant from differential approximants. We looked at approximants for $l \geq 9$ and $l - 3 \leq m \leq l + 3$. We have tabulated here 20 values which showed best convergence.
2. Table2:Estimates of critical exponents and growth constant from series analysis in three and four dimensions. Note that the value of θ and ν for rooted lattice animals/trees in $3d$ and $4d$ is known exactly(in $3d$, $\theta = \nu = 1/2$ and in $4d$, $\theta = 5/6$ and $\nu = 5/12$
3. Table3:Estimates of critical exponents and growth constants from Monte-Carlo simulations in four dimensions.

Figure Captions

1. Figure1: A rooted spiral tree of 15 sites on a square lattice. The root is the site enclosed in the square. At the root site the tree has freedom of choosing any of the four neighbouring sites. We count the spiral tree by number of sites and hence all bonds between two occupied sites is always assumed to be present. The site marked by X , if present will result in a loop for spiral site trees and hence will not be allowed. But it can be present in a spiral bond tree.
2. Figure2: Randomly generated spiral trees of 1000 sites in 2-dimensions using incomplete enumeration algorithm.
3. Figure3: A simple counting problem of backbone with arbitrary long offshoots. Minimum distance between two offshoots is 2 as else the tree constraint is violated. Solid squares represent the articulation points of the graph.
4. Figure4: An example of an irreducible spiral graph with no articulation point. This is also an example of a graph not included in $Q_1(x)$
5. Figure5: Schematic figure of spiral trees contributing to $B_i(x)$. $B_1(x)$ is just a single vertex.
6. Figure6: Example of graphs contributing to $V_i(x)$ and $W_i(x)$ respectively.
7. Figure7: Plot of $\frac{I_{pl,n}}{n^{2.312}}$ as a function of n for Monte-Carlo generated spiral trees on a square lattice.
8. Figure8: Plot of $I_{pl,n}$ Vs n for Monte-Carlo generated spiral trees on a square lattice. The dotted line is a straight line with slope 2.312.
9. Figure9: Monte-Carlo estimates of ratios of the number of configurations on a square lattice. The straight line gives a linear fit of the form $\lambda(1 - \theta/n)$ to the data.
10. Figure10: A spiral tree of six sites on a cubic lattice with a back-turn (drawn by a thicker line). This configuration will contribute to spiral trees ST_2 of six sites but not to ST_1 .

$[l, m]$	$x_c = 1/\lambda$	θ	$[l, m]$	$x_c = 1/\lambda$	θ
[14, 13]	0.47288256	-1.36083	[15, 18]	0.47307144	-1.39078
[14, 14]	0.47290325	-1.36384	[14, 17]	0.47307308	-1.39106
[15, 13]	0.47290516	-1.36413	[16, 17]	0.47307863	-1.39209
[16, 15]	0.47294898	-1.37035	[17, 15]	0.47308675	-1.39369
[13, 15]	0.47297513	-1.37499	[16, 19]	0.47309052	-1.39421
[16, 13]	0.47303007	-1.38409	[18, 15]	0.47310355	-1.39686
[13, 16]	0.47303305	-1.38436	[17, 18]	0.47310906	-1.39788
[16, 16]	0.47305593	-1.38800	[15, 16]	0.47311001	-1.39775
[14, 15]	0.47305793	-1.38863	[18, 18]	0.47311071	-1.39822
[15, 17]	0.47306712	-1.39002	[17, 19]	0.47311091	-1.39826

Table 1: Estimates of critical exponents and growth constant from differential approximants. We looked at approximants for $l \geq 9$ and $l - 3 \leq m \leq l + 3$. We have tabulated here 20 values which showed best convergence.

	$ST_1(d = 3)$	$ST_2(d = 3)$	$ST_1(d = 4)$	$ST_2(d = 4)$
λ	5.340 ± 0.020	5.683 ± 0.020	9.62 ± 0.10	10.20 ± 0.10
θ	-0.675 ± 0.050	-0.167 ± 0.050	-0.11 ± 0.10	0.29 ± 0.10
ν_{pl}	0.44 ± 0.05	0.477 ± 0.05	0.34 ± 0.05	0.37 ± 0.05
ν_{\perp}	0.54 ± 0.05	0.69 ± 0.05	0.44 ± 0.05	0.45 ± 0.05

Table 2: Estimates of critical exponents and growth constant from series analysis in three and four dimensions. Note that the value of θ and ν for rooted lattice animals/trees in $3d$ and $4d$ is known exactly(in $3d$, $\theta = \nu = 1/2$ and in $4d$, $\theta = 5/6$ and $\nu = 5/12$ [6].)

	$ST_1(d = 4)$	$ST_2(d = 4)$
λ	9.60 ± 0.1	10.2 ± 0.1
θ	-0.13 ± 0.1	0.17 ± 0.1
ν_{pl}	0.33 ± 0.02	0.38 ± 0.05
ν_{\perp}	0.451 ± 0.020	0.455 ± 0.050

Table 3: Estimates of critical exponents and growth constants from Monte-Carlo simulations in four dimensions.

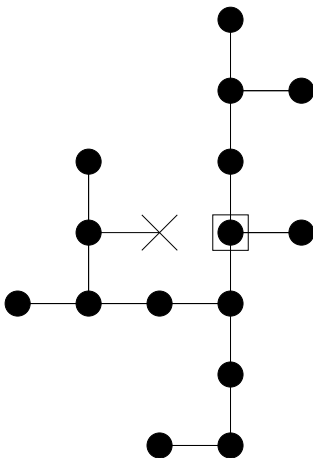


Figure 1: A rooted spiral tree of 15 sites on a square lattice. The root is the site enclosed in the square. At the root site the tree has freedom of choosing any of the four neighbouring sites. We count the spiral tree by number of sites and hence all bonds between two occupied sites is always assumed to be present. The site marked by X , if present will result in a loop for spiral site trees and hence will not be allowed. But it can be present in a spiral bond tree.

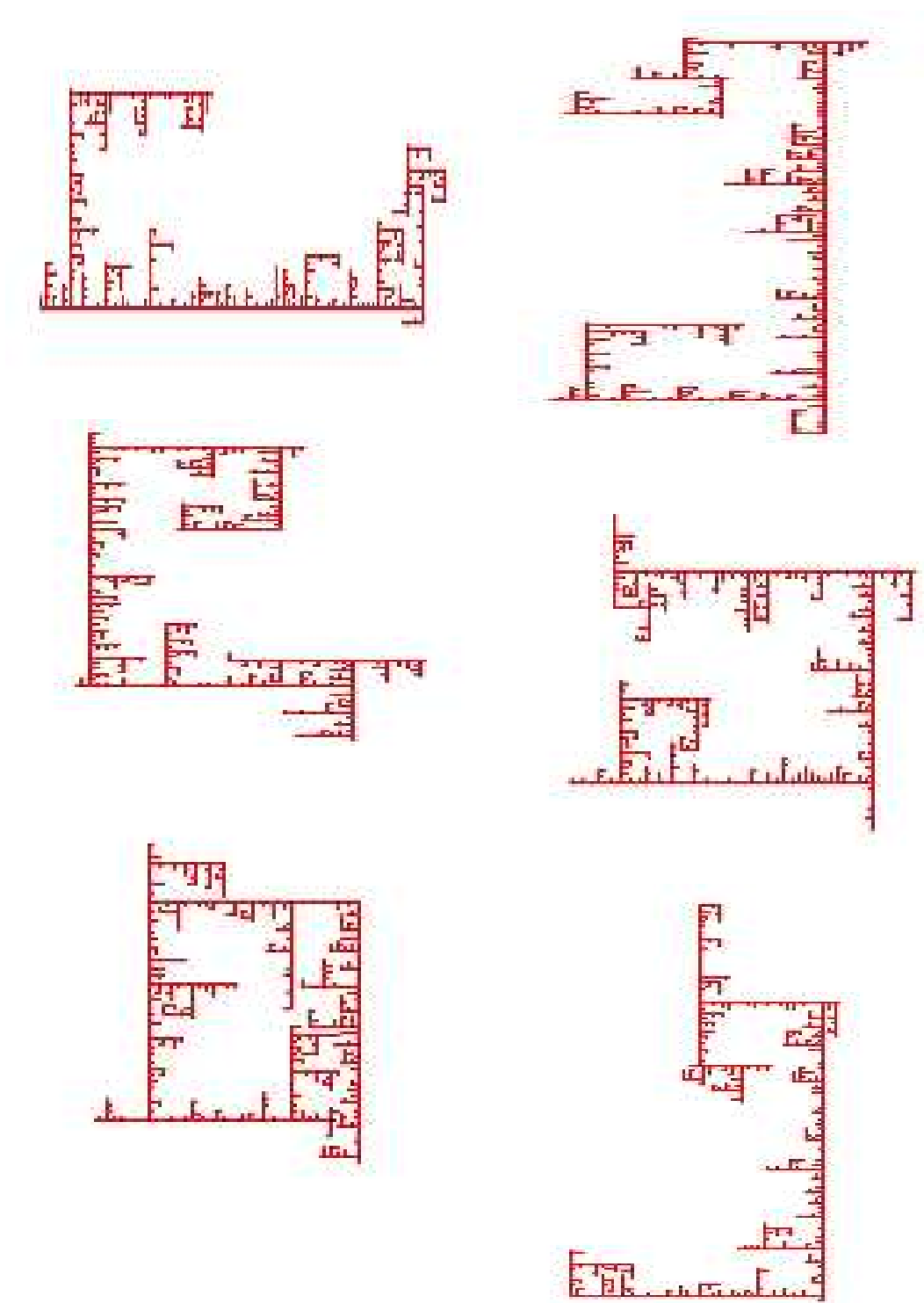


Figure 2: Randomly generated spiral trees of 1000 sites in 2-dimensions using incomplete-enumeration algorithm

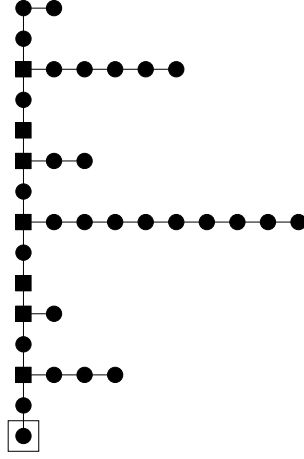


Figure 3: A simple counting problem of backbone with arbitrary long offshoots. Minimum distance between two offshoots is 2 as else the tree constraint is violated. Solid squares represent the articulation points of the graph.

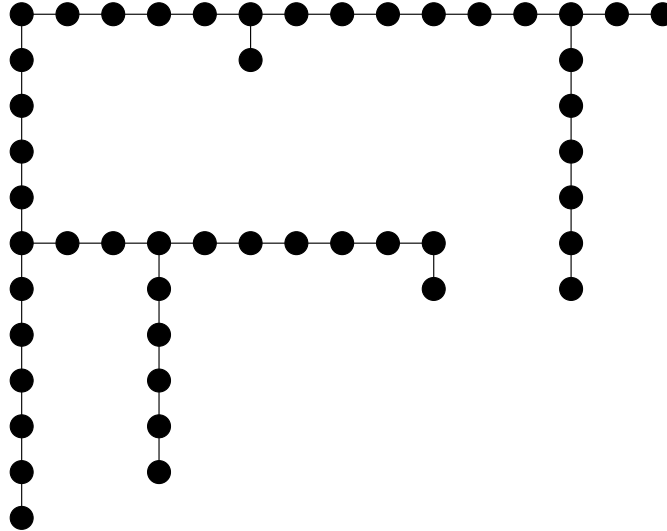


Figure 4: An example of an irreducible spiral graph with no articulation point. This is also an example of a graph not included in $Q_1(x)$

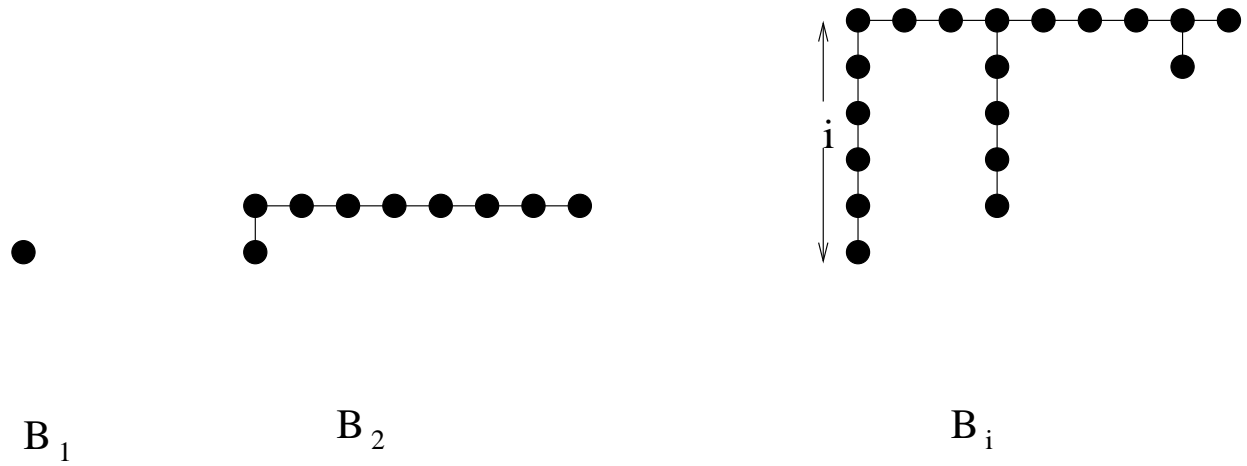


Figure 5: Schematic figure of spiral trees contributing to $B_i(x)$. $B_1(x)$ is just a single vertex.

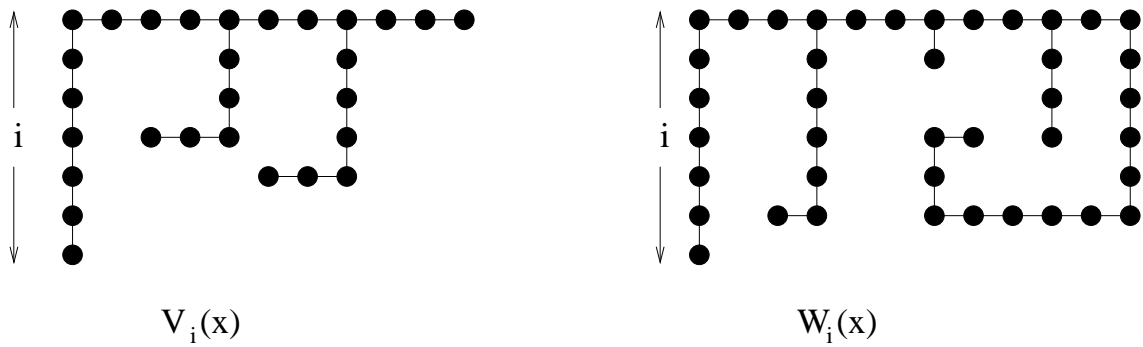


Figure 6: Example of graphs contributing to $V_i(x)$ and $W_i(x)$ respectively.

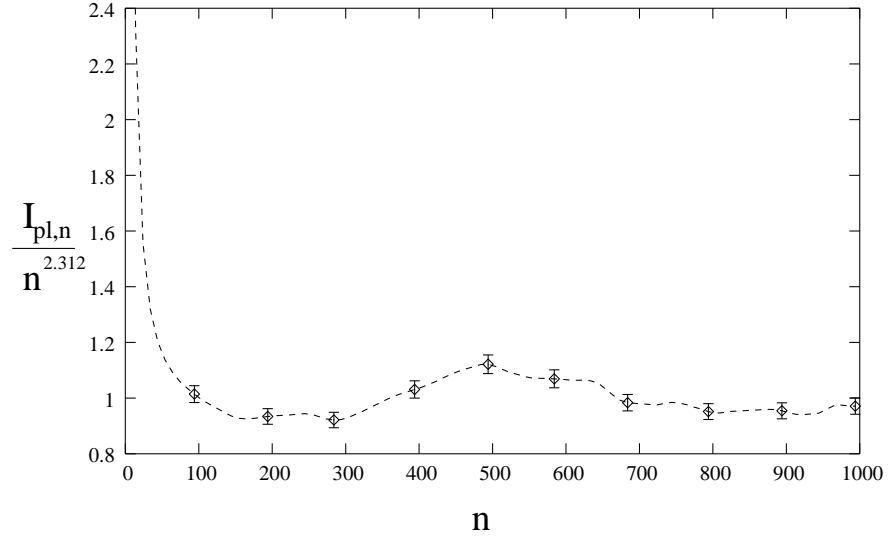


Figure 7: Plot of $\frac{I_{pl,n}}{n^{2.312}}$ as a function of n for Monte-Carlo generated spiral trees on a square lattice.

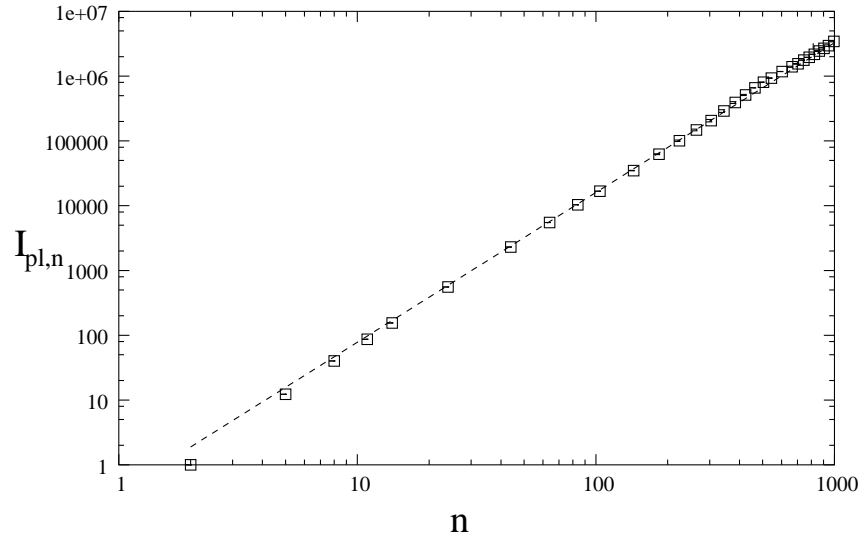


Figure 8: Plot of $I_{pl,n}$ Vs n for Monte-Carlo generated spiral trees on a square lattice. The dotted line is a straight line with slope 2.312.

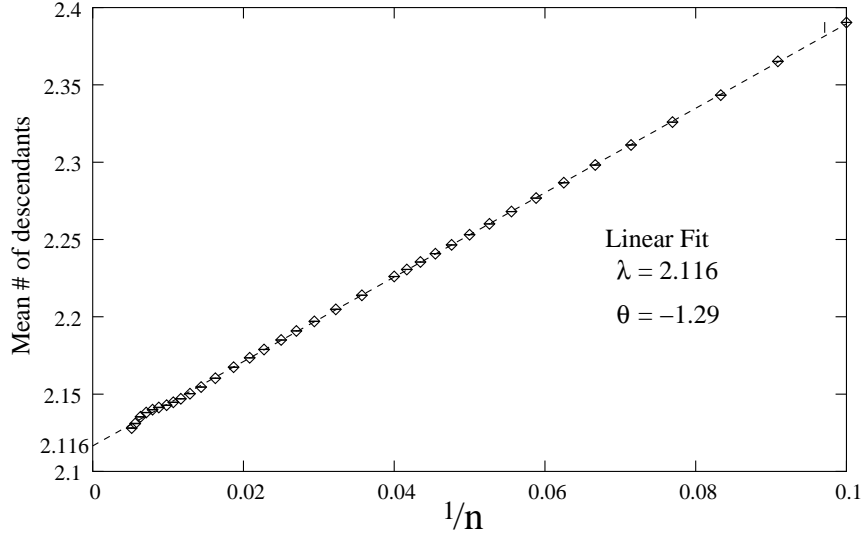


Figure 9: Monte-Carlo estimates of ratios of the number of configurations on a square lattice. The straight line gives a linear fit of the form $\lambda(1 - \theta/n)$ to the data.

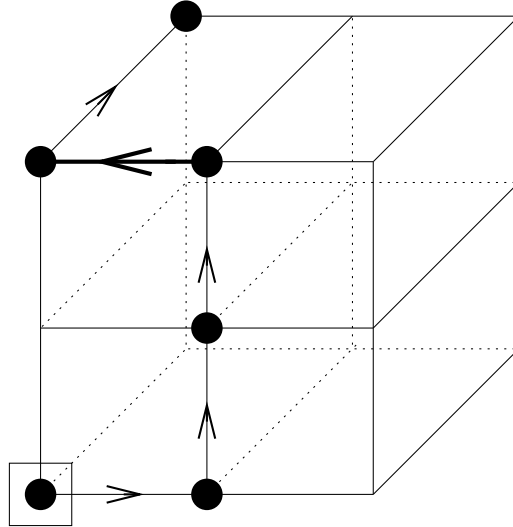


Figure 10: A spiral tree of six sites on a cubic lattice with a back-turn (drawn by a thicker line). This configuration will contribute to spiral trees ST_2 of six sites but not to ST_1 .